Journal of Thermal Spray and Engineering, Vol 5: 162-173
ISSN (Online): 2582-1474; DOI: https://doi.org/10.52687/2582-1474/501

The Indian Thermal Spray Association
ITSA ASSOCIATION FOR THERMAL SPRAY TECHNOLOGY AND RESEARCH

Peer-Reviewed

Prediction and Optimization of Mechanical Properties of HVOF Sprayed TiO2 Coatings Utilising Response Surface Methodology

R. Sathiyamoorthy[1], D. Thirumalaikumarasamy[2], R. Pradeep Raj[3]

[1]Government Polytechnic College, Bargur, Krishnagiri, Tamil Nadu -635104, India.

[2,3] Department of Manufacturing Engineering, Annamalai University, Chidambaram. Tamil Nadu – 608002, India.

ABSTRACT

The objective of this work is to optimise and estimate the porosity and hardness of HVOF-sprayed conventional TiO_2 coatings on magnesium alloys using Response Surface Methodology (RSM). The coatings were created to improve surface qualities including wear and corrosion resistance, which are essential for extending the life of magnesium alloys in a variety of industrial applications. A central composite design (CCD) was used to optimise important spray parameters such as oxygen flow rate, LPG flow rate, powder feed rate, and spray distance. The impact of these parameters on the porosity and hardness of TiO_2 coatings was thoroughly studied. Statistical models were created to correlate process variables with coating qualities, and the findings revealed a satisfactory fit between experimental and anticipated values. The results of the optimised conditions showed that Response Surface Methodology (RSM) is an effective predictive and optimisation technique for thermal spray operations, producing coatings with reduced porosity and increased hardness.

ARTICLE HISTORY
Received 03-12-2024
Revised 19-12-2024
Accepted 19-12-2024
Published 16-01-2025

KEYWORDS
HVOF spraying, TiO_2 coating, Mg alloy, Response Surface Methodology, Porosity, Hardness, Thermal spray optimization

Introduction

Thermal spraying is a versatile coating technique in which molten, semi-molten, or solid particles are propelled onto a substrate. The resulting coatings exhibit distinct microstructures and mechanical properties, making them suitable for a wide range of functional applications. The technology involves heating and accelerating feedstock particles using hot gas, flame, or plasma, which leads to the formation of a coating with a characteristic lamellar microstructure that significantly influences its properties [1]. To optimize coating characteristics for specific applications, precise control of operational spray parameters is essential. Statistical methods provide efficient approaches for experimental design and result analysis, ensuring comprehensive exploration of the experimental space [2]. The first step in experimental design involves selecting relevant process variables, which can range up to 50 in number. These variables typically fall into categories such as feedstock properties (e.g., size distribution, feed rate, morphology) and spray process parameters (e.g., gas flow rates, spray distance, particle size) [3].

Titania (TiO_2), a widely used industrial material, has promising applications in photocatalysis, electronics, optics, and tribology [4]. Thermal spray coatings made from titania offer excellent mechanical properties, making them resistant to wear from abrasion, erosion, and sliding [5]. While atmospheric plasma spraying is commonly employed for ceramics such as Al_2O_3, ZrO_2, and Cr_2O_3 due to their high melting points, the relatively lower melting point of TiO_2 (1855°C) enables the use of the High Velocity Oxygen Fuel (HVOF) process, which provides lower flame temperatures but higher particle velocities [6]. The properties of TiO_2 coatings are influenced by various physical and chemical conditions during the HVOF process, including pressure, temperature, and flame velocity. The primary process parameters affecting these conditions include oxygen flow rate, fuel flow rate, spray distance, and powder particle size. Due to the large number of tests required, traditional one-factor-at-a-time approaches for investigating these parameters are inefficient. This study presents a statistical design of experiments (DOE) approach to optimize the porosity and hardness of TiO_2 coatings on magnesium alloy and to examine the influence of HVOF spray process parameters. This methodology allows for the development of optimized coating processes by thoroughly exploring the experimental space and providing valuable insights into the relationships between process variables and coating properties.

Experimental

Materials

Commercially available pure Titanium sheets of 2.5mm thickness were used as a substrate in this investigation. Fig.1 shows the optical microstructure of the titanium substrate and reveals the equiaxed grains. Table 1 details the chemical composition of the titanium substrate. The chemical composition of titanium was determined using inductively coupled plasma–optical emission spectroscopy (Metax Lab, Chennai).

Table 1: Chemical composition of Titanium (wt %)

Al	Sn	Fe	Cr	V	Ti
0.0035	0.0195	0.04425	0.00287	0.03737	Remaining

For this study, fused and crushed titanium oxide (TiO_2) and silicon carbide (SiC) were used as coating materials. TiO_2

Corresponding Author: R. Sathiyamoorthy, Tel: +91 6381761102
Email: rsmoorthy32@gmail.com
Contents lists available at http://www.inscience.in/JTSE.html

was sourced from H.C. Stark AMPERIT, and SiC was obtained from M/S Metallizing Equipment Co. Pvt Ltd, Jodhpur. As illustrated in Fig. 2 the scanning electron microscopy (SEM) images of TiO_2 and SiC feedstocks reveal their angular and blocky morphologies.

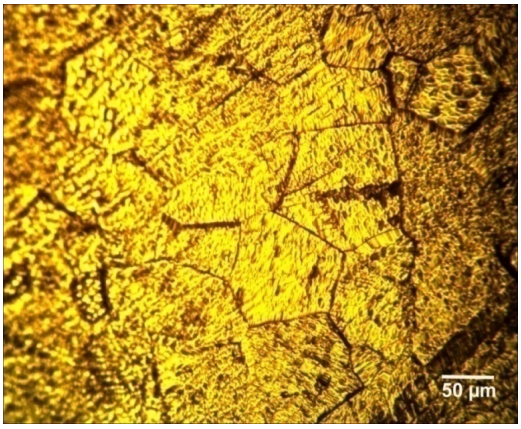

Figure 1: Optical Microstructure of Titanium

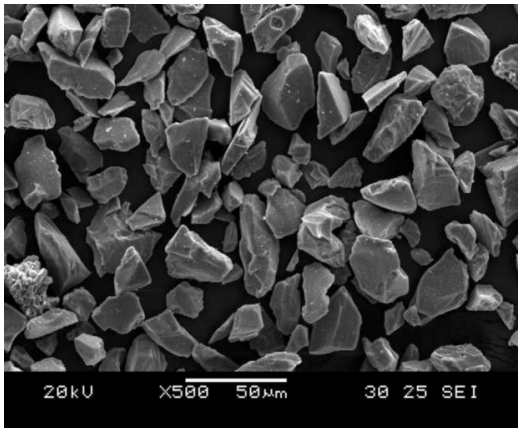

(a)

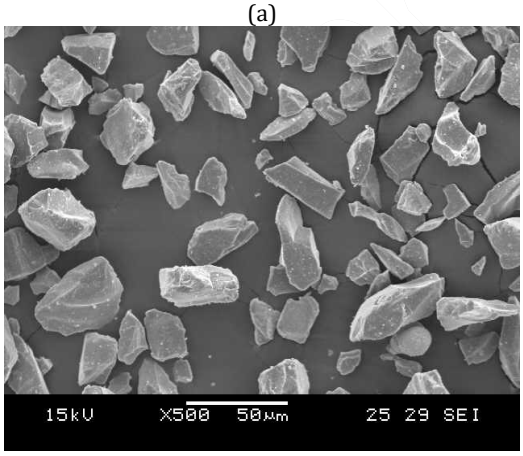

(b)

Figure 2: SEM morphology of TiO_2 and SiC and Powders

A high-energy ball milling procedure was used to create composite feedstocks using TiO_2 and different percentages of SiC (5%, 10%, and 15%). Using tungsten carbide balls, the powder combination was added to a jar until it reached 25% of its total volume, ensuring a 1:1 ball-to-weight ratio. For one hour, the milling procedure was carried out at 150 rpm. After that, the powder was put through a vibrating sieve to extract feedstock particles that ranged in size from 10 to 30 µm. These particles were then utilised straight for spraying. The titania-silicon carbide blended feedstock's scanning electron microscope (SEM) morphology is shown in Figure 3. Figure 4 shows the results of an X-ray diffraction (XRD) study of the TiO_2 feedstock. It shows that anatase is the main phase, with rutile present in trace levels. The phase composition has a considerable influence on the coating's qualities. Anatase's metastability and low-density lead to increased photocatalytic activity and corrosion resistance due to its higher surface energy. However, it is less mechanically resistant than rutile. On the other hand, the rutile phase, which is thermodynamically stable and denser, improves the coating's hardness and wear resistance but may reduce its corrosion resistance and photocatalytic efficacy. Therefore, an enhanced rutile concentration in the coating would favour applications requiring better mechanical endurance, but coatings rich in anatase are more suitable for situations demanding superior corrosion protection. Figure 5 shows the XRD pattern of the SiC feedstock.

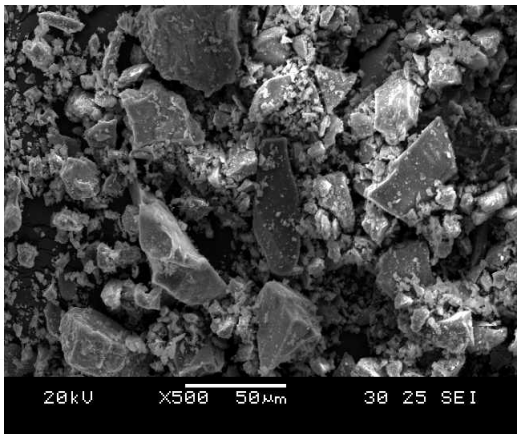

Figure 3: SEM Morphology of TiO_2 with SiC blended feedstock

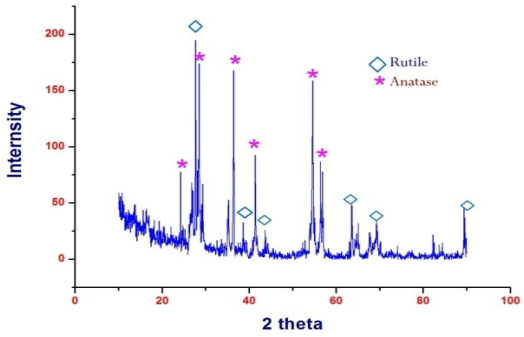

Figure 4: XRD analysis of TiO_2 feedstock

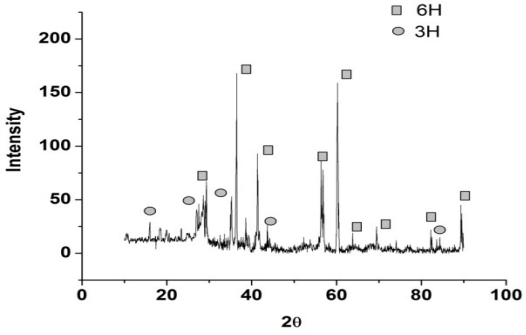

Figure 5: XRD of SiC feedstock

HVOF spraying of TiO_2 and TiO_2 + SiC Coating

HVOF spraying was conducted using a system from M/S Metallising Equipment Co. Pvt. Ltd., Jodhpur, India. This technology utilizes a mixture of oxygen and liquefied petroleum gas (LPG) to generate a supersonic jet. The spray parameters, initially optimized for TiO_2 coatings, were subsequently applied to all SiC composite coatings. The spray distance was maintained as a constant process parameter throughout the coating procedure. Titanium specimens were prepared by cutting from the original material and subjected to grit blasting using 500 to 320 µm corundum grits. The surface roughness of the specimens was measured with a surface roughness tester (Mitutoyo, Japan; model Surf Test 301), revealing an average roughness of 5–10 µm, following cleaning with acetone in an ultrasonic bath and subsequent drying. Figures 6 and 7 illustrate the HVOF spraying system and spraying gun, respectively.

Figure 6: HVOF Spraying system

Figure 7: HVOF Spray gun

The coating thickness of the coatings measured using a digital micrometer with an accuracy of 0.001mm, the average thickness of the coatings measured in this study was 200 -250 µm.

Coating Characterization

The metallographic cross-sections of the coatings were prepared to evaluate porosity and microhardness. Each specimen, measuring 10x10 mm, was sectioned using a slow-speed metallurgical saw to ensure precision. The samples were then mounted in epoxy resin under vacuum conditions. Grinding and polishing were performed in stages using silicon carbide papers and diamond slurries to achieve a smooth finish. Due to the brittle nature of ceramic coatings, careful attention was paid to prevent artifacts from grinding and polishing, as material loss can create the appearance of increased porosity. To minimize these effects, both surface and cross-sectional microstructures were examined using an optical microscope. Porosity was quantified according to ASTM B276 standards, utilizing an optical microscope with image analysis capabilities. Multiple random locations across the polished cross-section were analyzed at 400x magnification, using a 200 µm square area for each image. The porosity percentage was determined by averaging the results from these images.

The microhardness of the coatings was evaluated using a Vickers Microhardness tester (Shimadzu, Japan, Model: HMV-2T). A load of 300 g was applied for a dwell time of 15 seconds. Measurements were taken at 10 randomly selected points on the polished cross-section of the coating to ensure a representative hardness profile.

Developing the experimental design matrix.

To optimise the process of producing highly adherent HVOF spray coatings, a central composite rotatable design matrix with four elements and five levels was used. This architecture, which is central to response surface methodology (RSM), is very effective at developing empirical models that characterise the relationship between process parameters and the resulting response surfaces. Additionally, it reduces the number of experiments needed, making it a cost-effective and time-saving approach for process optimization. [7]. Table 2 presents the key parameters and their corresponding levels.

Table 2: Important HVOF spray parameters and their levels

No	Factor	Units	Levels				
			-2	-1	0	1	2
1	Oxygen Flow Rate (O)	Lpm	252	256	260	264	268
2	LPG Flow Rate (F)	Lpm	62	66	70	74	78
3	Powder Feed Rate (P)	g/min	28	33	38	43	48
4	Spray Distance (D)	Mm	216	222	228	234	240

The study involved the preparation of 30 TiO_2 coatings using various HVOF spraying parameters, as detailed in the experimental design matrix (Table 3). To reduce systematic errors, the experiments were performed in a randomized sequence. Titanium specimens, each measuring 25 mm × 25 mm × 2 mm, were pretreated by grit blasting with

Table 3: Design matrix and experimental results

S. No.	Coded value				Original values				Responses	
	Oxygen flow rate (lpm)	LPG flow rate (lpm)	Powder feed rate (gpm)	Spray distance (mm)	Oxygen flow rate (lpm)	LPG flow rate (lpm)	Powder feed rate (gpm)	Spray distance (mm)	Coating Porosity (Vol %)	Coating Hardness ($HV_{0.3}$)
1	-1	-1	-1	-1	256	66	33	222	4	750
2	1	-1	-1	-1	264	66	28	222	2.65	845
3	-1	1	-1	-1	256	74	33	222	2.69	825
4	1	1	-1	-1	264	74	33	222	2.32	898
5	-1	-1	1	-1	256	66	43	222	4.72	739
6	1	-1	1	-1	264	66	43	222	2.62	829
7	-1	1	1	-1	256	74	43	222	2.37	880
8	1	1	1	-1	264	74	43	222	2.6	867
9	-1	-1	-1	1	256	66	33	234	4.37	779
10	1	-1	-1	1	264	66	33	234	1.86	917
11	-1	1	-1	1	256	74	33	234	4	776
12	1	1	-1	1	264	74	33	234	3	840
13	-1	-1	1	1	256	66	43	234	5	658
14	1	-1	1	1	264	66	43	234	4.5	740
15	-1	1	1	1	256	74	43	234	4.6	730
16	1	1	1	1	264	74	43	234	3.87	778
17	-2	0	0	0	252	70	38	228	4.56	721
18	2	0	0	0	268	70	38	228	2.8	859
19	0	-2	0	0	260	62	38	228	4.57	712
20	0	2	0	0	260	78	38	228	2.94	824
21	0	0	-2	0	260	70	28	228	2.53	871
22	0	0	2	0	260	70	48	228	4.59	792
23	0	0	0	-2	260	70	38	216	2.94	874
24	0	0	0	2	260	70	38	240	4.54	746
25	0	0	0	0	260	70	38	228	2.17	891
26	0	0	0	0	260	70	38	228	2.24	896
27	0	0	0	0	260	70	38	228	2.17	887
28	0	0	0	0	260	70	38	228	2.8	893
29	0	0	0	0	260	70	38	228	2.06	886
30	0	0	0	0	260	70	38	228	2.14	898

corundum grits (particle size: 500 to 320 µm), followed by ultrasonic cleaning in acetone. After grit blasting, the surface roughness was measured to be 5 µm using a surface roughness tester (Mitutoyo, Japan; model Surf Test 301). Porosity analysis was conducted on the polished cross-sections of the coatings in accordance with ASTM B276 standards. An optical microscope (MEIJI, Japan; Model: MIL-7100) equipped with image analysis software was employed for this purpose. Microhardness testing was carried out using a Vickers microhardness tester (Shimadzu, Japan; Model: HMV-2T) with a 300 g load and a 15-second dwell time. Microhardness was measured at ten randomly selected points on the polished cross-sections.

In this study, the response porosity and microhardness of the HVOF sprayed coating were predicted using the response surface approach. Response surface methodology (RSM), which is helpful for creating, refining, and optimising HVOF process, is a combination of statistical and mathematical methodologies based on a few tests [8]. In order to forecast the outcomes of trials involving various combinations, a second order quadratic model was created. The reactions can be described as a function of the Spray distance (D), Powder feed rate (P), LPG flow rate (F), and Oxygen flow rate (O).

$$Responses = f(O, F, P, D) \quad (1)$$

The general form of a quadratic model in several parameters is:

$$Y = bo + \sum bixi + \sum bii\, x^2 + \sum bij\, xi\, xj \quad (2)$$

For the four factors, the selected polynomial equation can be expressed as

$$Y = bo + b1\,(O) + b2(F) + b3(P) + b4(D) + b11(O^2) + b22\,(F^2) + b33(P^2) + b44(D^2) + b12(OF) + b13(OP) + b14(OD) + b23\,(FP) + b24(FD) + b34(PD) \quad (3)$$

The average of the responses is denoted by bo, while the regression coefficients b1, b2, b3,.....b44 are determined by the corresponding linear, interaction, and square terms of the factors. The Design Experiment software was used to calculate the coefficient's value. The final empirical relationship was created utilising the coefficients that were determined (with a 95% confidence level). Equation 4 and 5 is the final statistical model used to estimate the responses:

$$Coating\ Porosity = \{2.2 - 0.4O - 0.31F + 0.39\,P + 0.43O\,D + 0.28OF + 0.13\,C\,O - 0.07\,DF - 0.15\,FP + 0.23\,D\,P + 0.25\,D + 0.31\,O^2 + 0.33\,F^2 + 0.28\,P^2 + 0.32\,D^2\}\ vol\% \quad (4)$$

$$Coating\ Hardness = \{891.8 + 35.5O + 27.5F - 19.4\,P - 32.1\,D - 8.3\,OF - 3.9\,OP - 0.81\,OD + 15\,FP - 17.3\,FD - 25.2\,PD - 24.9O2 - 30.4\,F^2 + 14.5\,P^2 - 19.9\,D^2\}HV \quad (5)$$

Table 4: ANOVA test results for the response Coating Hardness

Source	Sum of Squares	df	Mean Square	F Value	Prob > F	
Model	145414.6	14	10386.75	339.8683	< 0.0001	Significant
O-O	30317.04	1	30317.04	992.0137	< 0.0001	
F-F	18205.04	1	18205.04	595.6931	< 0.0001	
P-P	9087.042	1	9087.042	297.34	< 0.0001	
D-D	24768.38	1	24768.38	810.454	< 0.0001	
OF	1105.563	1	1105.563	36.17547	< 0.0001	
OP	248.0625	1	248.0625	8.116933	0.0122	
OD	10.5625	1	10.5625	0.345619	0.5654	
FP	3630.063	1	3630.063	118.7804	< 0.0001	
FD	4795.563	1	4795.563	156.9172	< 0.0001	
PD	10150.56	1	10150.56	332.1398	< 0.0001	
O^2	17014.53	1	17014.53	556.7378	< 0.0001	
F^2	25358.81	1	25358.81	829.7739	< 0.0001	
P^2	5791.741	1	5791.741	189.5134	< 0.0001	
D^2	10868.81	1	10868.81	355.6419	< 0.0001	
Residual	458.4167	15	30.56111			
Lack of Fit	343.5833	10	34.35833	1.496009	0.3436	Not significant
Pure Error	114.8333	5	22.96667			
Corrected Total	145873	29				
Std deviation	5.52821		R-Squared	0.996857		
Mean	820.0333		Adj R-Squared	0.993924		
CV %	0.674145		Pred R-Squared	0.9853		
			Adeq Precision	67.29069		

CV: coefficient of variance; F: Fisher Ratio; p: probability; df: degree of freedom

Table 5: ANOVA test results for the response Coating porosity

Source	Sum of Squares	Df	Mean Square	F Value	p-value prob>F	
Model	28.22995	14	2.016425	13.22665	< 0.0001	Significant
O-O	5.850938	1	5.850938	38.37897	< 0.0001	
F-F	2.362538	1	2.362538	15.49696	0.0013	
P-P	3.768338	1	3.768338	24.71824	0.0002	
D-D	4.532704	1	4.532704	29.73207	< 0.0001	
OF	1.316756	1	1.316756	8.637205	0.0102	
OP	0.283556	1	0.283556	1.859975	0.1927	
OD	0.082656	1	0.082656	0.54218	0.4729	
FP	0.400056	1	0.400056	2.624151	0.1261	
FD	0.878906	1	0.878906	5.765147	0.0298	
PD	1.045506	1	1.045506	6.857952	0.0194	
O^2	2.7198	1	2.7198	17.84041	0.0007	
F^2	3.053336	1	3.053336	20.02822	0.0004	
P^2	2.226257	1	2.226257	14.60304	0.0017	
D^2	2.985086	1	2.985086	19.58054	0.0005	
Residual	2.286775	15	0.152452			
Lack of Fit	1.924242	10	0.192424	2.653882	0.1465	Not significant
Pure Error	0.362533	5	0.072507			
Cor Total	30.51672	29				
Std. Dev.	0.390451		R-Squared	0.925065		
Mean	3.274		Adj R-Squared	0.855125		
C.V. %	11.9258		Pred R-Squared	0.619694		
			Adeq Precision	12.04316		

CV: coefficient of variance; F: Fisher Ratio; p: probability; df: degree of freedom

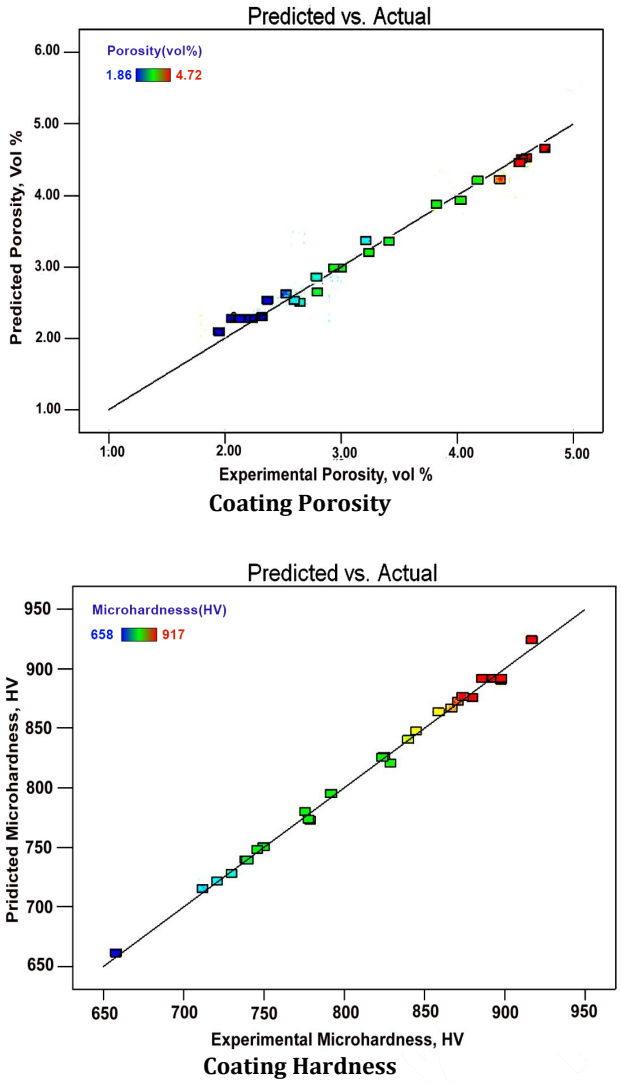

Figure 8: Correlation Graph

Checking the adequacy of the developed model

The generated empirical model was evaluated for adequacy using Analysis of Variance (ANOVA) [9]. There was a 95% confidence interval. When the computed R-ratio exceeded the tabulated R-ratio for the appropriate confidence level and the calculated F-ratio did not exceed the tabulated F-ratio, the model was considered adequate. The low probability value (p-model>F = 0.0001) from Fisher's F-test supported the importance of the model. With regard to all of the established empirical links, lack of fit was not significant. The coefficient of determination (R^2) and the adjusted coefficient of determination were used to assess the model's goodness of fit. Since both values were higher than 0.99, the model was able to account for less than 1% of the variation in total. Adequate precision was assessed by comparing the range of predicted values at design points with the average prediction error. The high correlation between estimated and predicted values, as shown in Fig. 8, further supports the model's accuracy.

Results and Discussion

The developed model demonstrates the ability to optimize responses and generate parametric research charts. The perturbation graph (Fig. 9) provides insights into the interaction of HVOF process parameters with coating porosity and microhardness. The graph illustrates how the response changes when a single parameter deviates from a reference point, while others remain constant. A flat line in the graph indicates insensitivity to a parameter, whereas a steep slope denotes sensitivity [10,11]. According to the Analysis of Variance (ANOVA), porosity and hardness are primarily influenced by spray distance and LPG flow rate. The perturbation plot further confirms this trend, revealing that porosity decreases with increasing process parameters up to an optimal point, after which it increases. At lower fuel flow rates, inadequate particle melting occurs due to insufficient flame temperature, resulting in high porosity and low hardness. Since the melting point of TiO_2 is 1855°C, the flame temperature at low fuel rates becomes insufficient to ensure droplet deformation and complete void filling, which adversely impacts coating quality.

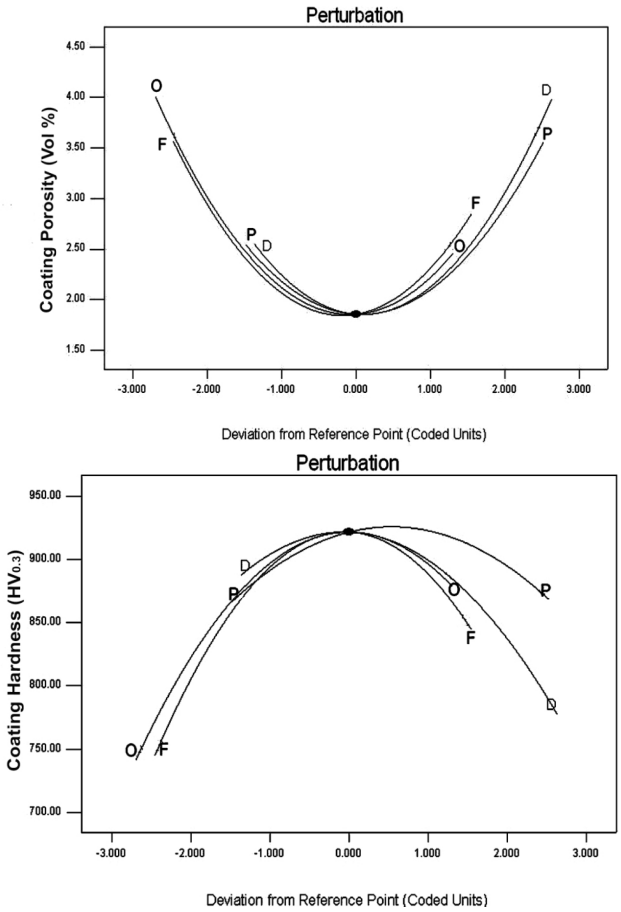

Figure 9: Perturbation graph

Conversely, higher fuel gas flow rates can elevate flame temperature by adjusting oxygen flow and pressure, enhancing particle melting and droplet deformation. This improvement results in increased inter-splat contact, decreased droplet viscosity, and subsequently reduced porosity and higher microhardness [12,13]. However, excessively high fuel flow rates can cause undesired effects such as gas entrapment during particle impact and premature melting of Titania particles. Rapid quenching and gas bubble formation within the splats can generate localized pressure, increasing porosity and reducing microhardness [14].

The graph further highlights the role of oxygen flow rate in determining flame temperature and velocity during HVOF spraying. Complete combustion of LPG in the presence of adequate oxygen achieves the highest flame temperature. However, excessive oxygen flow can act as a coolant, lowering flame temperature and reducing particle residence time [15]. Conversely, insufficient oxygen results in incomplete combustion, thereby lowering flame temperature. Both extremes lead to unmelted particles that fail to adhere properly to the substrate, increasing rebound effects, porosity, and reducing coating hardness [16]. The influence of powder feed rate (curve F in Fig. 9) on coating responses is also significant. Variations in powder feed rate alter particle temperature and velocity, as particles compete for the flame's thermal and kinetic energy. At relatively low powder feed rates, most particles undergo complete melting; however, rapid quenching can cause cracks, which increase porosity and reduce hardness. Conversely, an optimal powder feed rate promotes sufficient particle melting, enhancing hardness and reducing porosity [17].

As shown in Fig. 9 (curve D), coating hardness initially increases with spray distance but eventually declines. At longer spray distances, reduced particle velocity upon impact leads to coatings with lower density. Additionally, lower impact temperatures increase the proportion of unmelted particles, further contributing to porosity. Atmospheric drag at extended spray distances decelerates ceramic particles, reducing their enthalpy and preventing effective deformation upon impact [18]. In contrast, shorter spray distances increase deposition rates but may introduce excessive heat loads, causing quenching cracks and reducing coating hardness. An optimal spray distance ensures that the gas jet imparts sufficient thermal energy and velocity to the particles, enabling cohesive splat packing, thereby minimizing porosity and maximizing hardness [19]. The dependability of each parameter, including their covariance, is critical for understanding the combined influence on coating properties. Spray distance, fuel flow rate, and oxygen flow rate exhibit interdependence, where a change in one parameter can affect the performance of the others. For instance, increasing fuel flow rate without optimizing oxygen flow may lead to incomplete combustion, negating the benefits of higher flame temperatures. Similarly, variations in spray distance can influence particle residence time, which is inherently tied to powder feed rate and flame velocity. Covariance analysis can provide a deeper understanding of these interrelationships, offering valuable insights into process stability and parameter optimization. Such an analysis ensures that the combined effect of parameters is considered, leading to reliable and reproducible coating characteristics.

Optimizing HVOF spray parameters

The surface response was estimated to determine the optimal parameter values. Characterizing how the significant factors influence the response is essential for optimization purposes. Additionally, setting a target to enhance the responses of interest is critical for improving outcomes. The quadratic response equation for porosity is represented as a solid surface in the two-dimensional contour plots (Fig. 10(a-f)) and three-dimensional response surfaces (Fig. 11(a-f)). Similarly, the quadratic response equation for hardness is depicted in the two-dimensional contour plots (Fig. 12(a-f)) and three-dimensional response surfaces (Fig. 13(a-f)).

These response contours enable the prediction of porosity and hardness within any zone of the experimental domain [20]. To visually represent the ideal factor settings, a contour map is generated. For second-order models, this plot can be more complex than the straightforward parallel lines typically seen in first-order models. Upon identifying a stationary point, it is crucial to analyze the response surface near this point. Characterizing whether the stationary point represents a saddle point, minimum response, or maximum response is an integral part of the process. Contour plots play a vital role in examining the response surface [21].

According to Fig. 13, porosity decreases, troughs, and then rises when the values of the process parameters under consideration rise. The response plot's valley displays the least amount of porosity. Based on the response graph, effective factors influencing porosity were LPG fuel flow and spray distance. At the optimal fuel flow rate, the flame attains higher temperatures and velocities. At the same time, the optimal spray distance facilitates the effective deposition of TiO_2 particles onto the substrate. As a result, interlamellar porosity and the fraction of unmelted particles were reduced.

The SEM image of the TiO_2 coating surface (Figure 14) reveals distinct evidence of particle agglomeration at higher fuel flow rates. This is characterized by the presence of large, irregular particle clusters, which disrupt the uniformity of the coating surface. Additionally, the appearance of voids and inter-particle gaps indicates incomplete fusion or improper deposition of particles, likely caused by the excessive velocity or temperature fluctuations at higher fuel flow. Non-uniform particle distribution across the coating further supports this observation, as regions with denser agglomerates suggest localized accumulation of particles.

Furthermore, the presence of larger agglomerated particles, as opposed to finely dispersed structures, highlights the adverse impact of increased fuel flow on deposition quality. These morphological features collectively suggest that higher fuel flow rates hinder effective particle control, leading to agglomeration and compromising the overall quality of the TiO_2 coating. Under optimal conditions, the coating exhibits a dense, interconnected structure. Porosity significantly influences microhardness, with lower porosity resulting in higher density.

Contour plots and 3D response surfaces from the regression model indicate that the maximum hardness corresponds to the apex of the response. Increasing levels of the factors considered generally lead to a decrease in hardness. The overlay plots generated from graphical optimization are practical tools for TiO_2 coating manufacturers to select HVOF spray parameters that achieve desired hardness values. The yellow shaded areas in the overlay plot (Figure 15F) represent regions that meet the specified criteria and optimized conditions. Microhardness of the TiO2 coating was found to range from 730 HV0.3 to 922 HV0.3, with optimal conditions yielding dense and harder coatings.

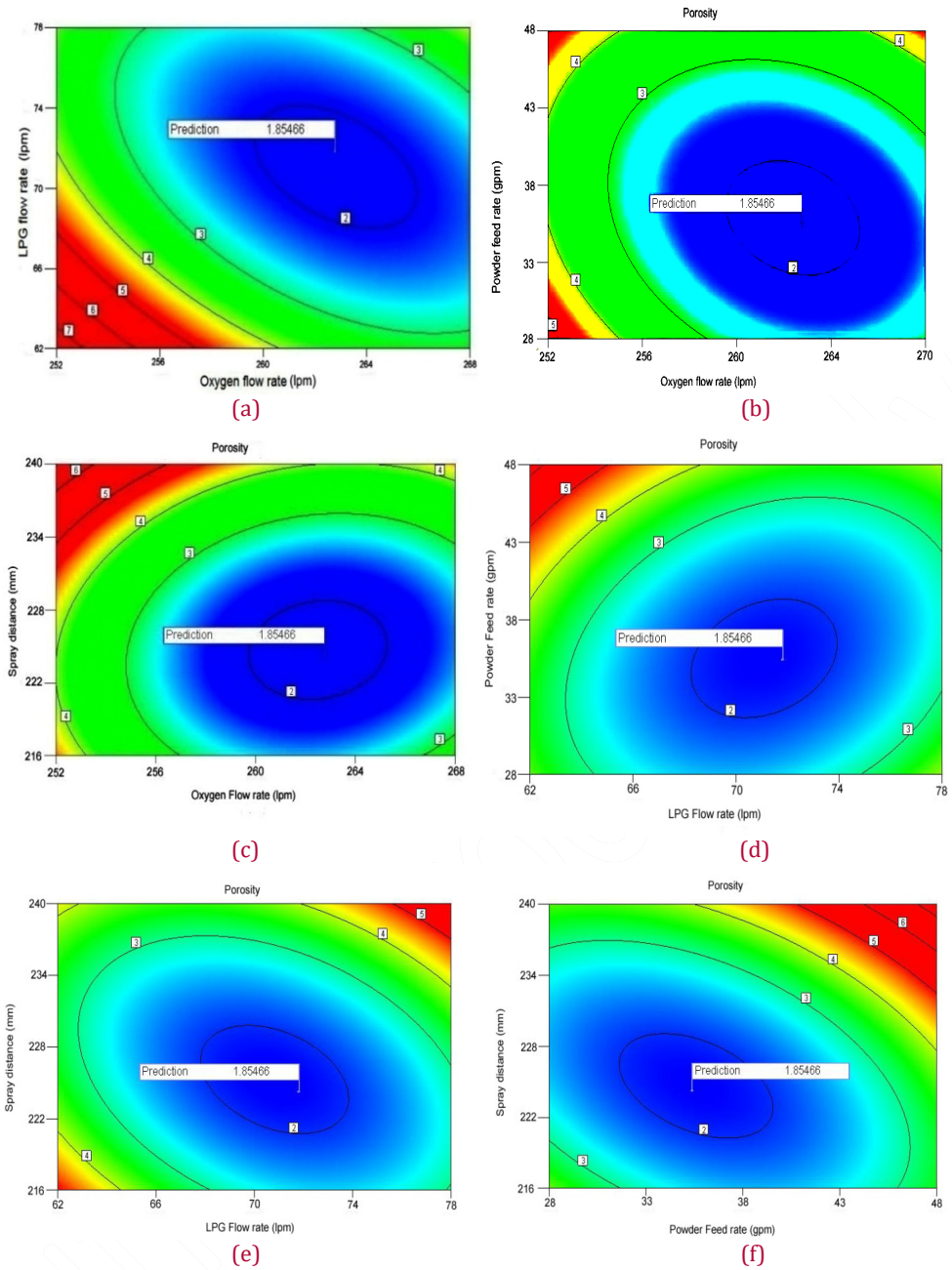

Figure 10: Contour plots for response coating porosity Effect of (a) O2 flow rate and Fuel flow rate, (b) O2 flow rate and Powder feed rate, (c) O2 flow rate and spray distance, (d) Fuel flow rate and powder feed rate, (e) Fuel flow rate and spray distance, (f) powder feed rate and spray distance

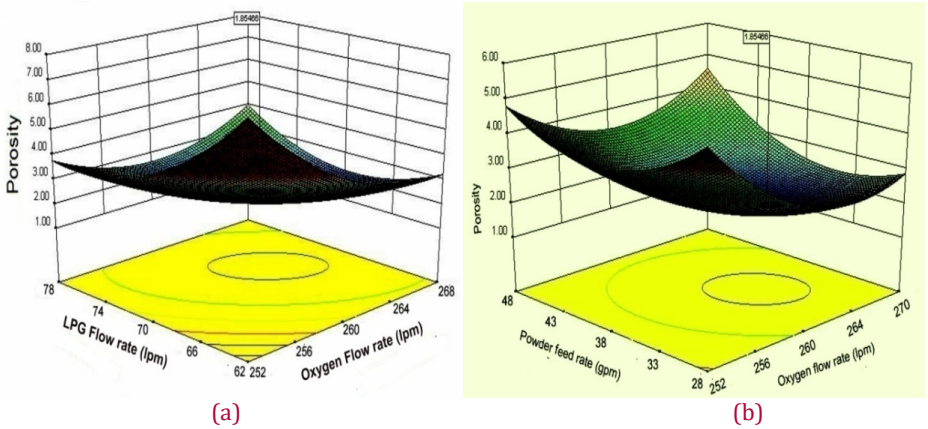

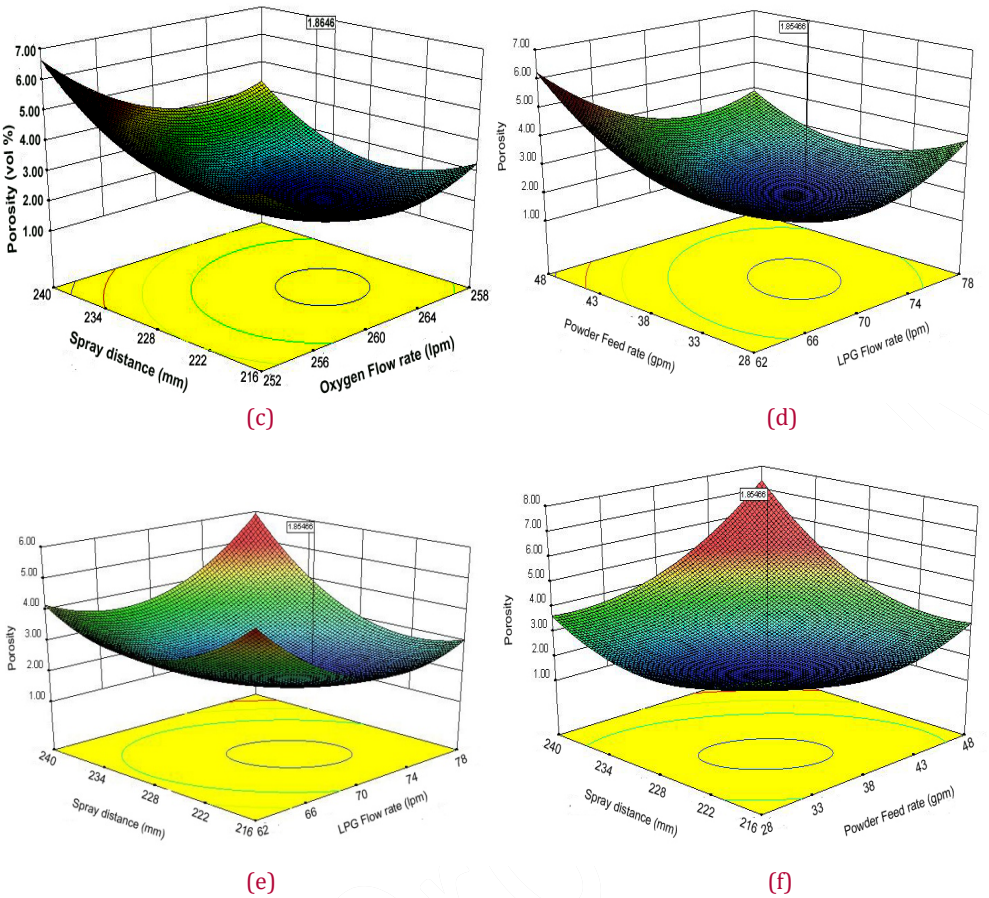

(c) (d)

(e) (f)

Figure 11: Response graphs for coating porosity, Effect of (a) O_2 flow rate and Fuel flow rate, (b) O_2 flow rate and Powder feed rate, (c) O_2 flow rate and spray distance, (d) Fuel flow rate and powder feed rate, (e) Fuel flow rate and spray distance, (f) powder feed rate and spray distance

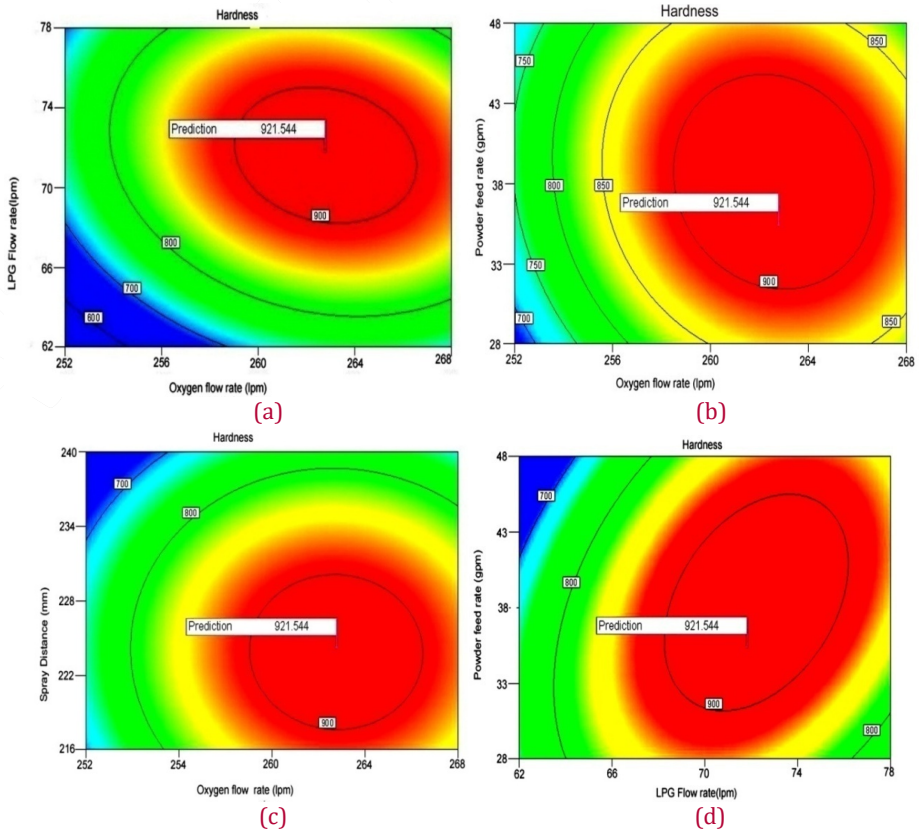

(a) (b)

(c) (d)

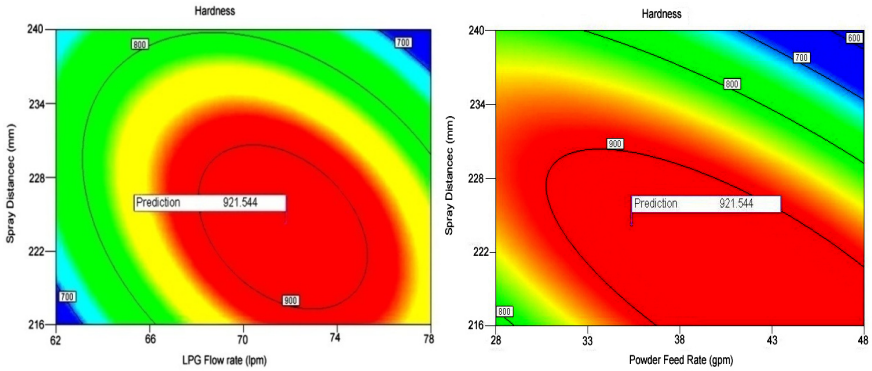

(e) (f)

Figure 12: Contour plots for response coating hardness, (a)Effect of O_2 flow rate and Spray distance on coating hardness , (b)Effect of O_2 flow rate and powder feed rate on coating hardness , (c)Effect of O_2 flow rate and spray distance on coating hardness , (d)Effect of fuel flow rate and powder feed rate on coating hardness , (e)Effect of fuel flow rate and spray distance on coating hardness , (f)Effect of fuel powder feed rate and spray distance on coating hardness

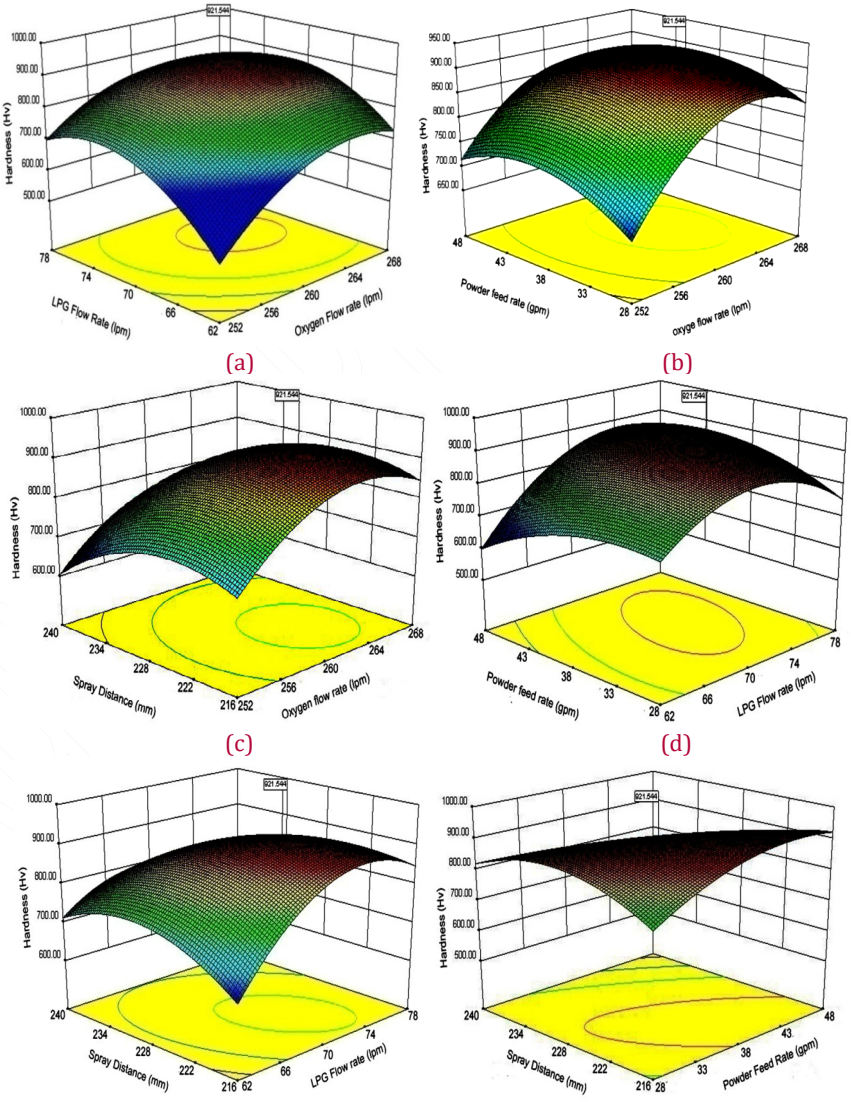

(a) (b)

(c) (d)

(e) (f)

Figure 13: Response graphs for coating hardness, (a)Effect of O_2 flow rate and Spray distance on coating hardness , (b)Effect of O_2 flow rate and powder feed rate on coating hardness, (c)Effect of O_2 flow rate and spray distance on coating hardness , (d)Effect of fuel flow rate and powder feed rate on coating hardness, (e)Effect of fuel flow rate and spray distance on coating hardness , (f)Effect of fuel powder feed rate and spray distance on coating hardness

Contents lists available at http://www.inscience.in/JTSE.html

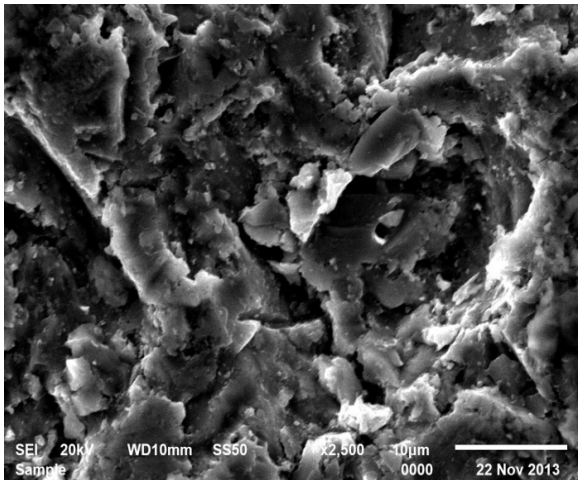

Figure 14: SEM morphology of top surfaces of TiO_2 coating

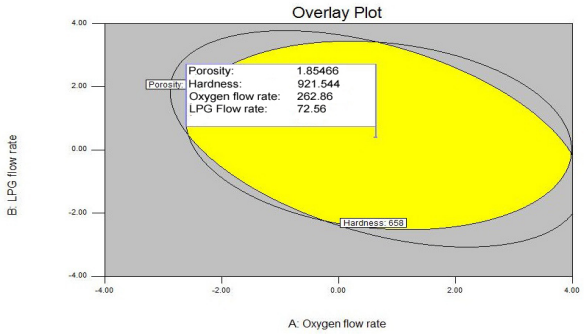

Figure 15: Overlay plot

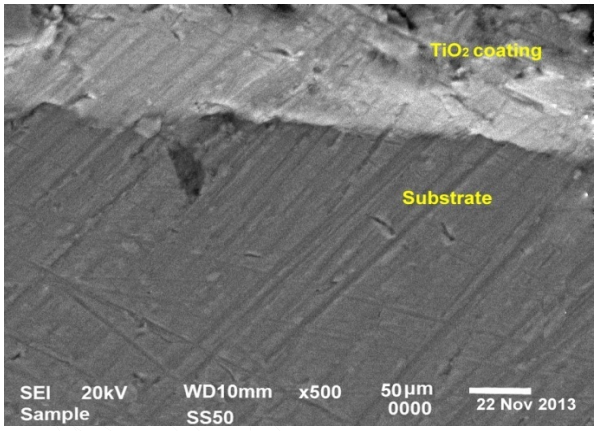

Figure 16: SEM image of TiO_2 coating cross-section

Greater particle temperatures, resulting from higher flame jet temperatures, can reduce porosity by enhancing cohesiveness and increase hardness [22]. Through numerical optimization, which involved solving equations 4 and 5, analyzing response surfaces, and creating contour plots, the following optimal parameter settings were determined: an oxygen flow rate of 262.82 liters per minute (lpm), an LPG flow rate of 72.56 lpm, a powder feed rate of 39.24 grams per minute (gpm), and a spray distance of 229.78 millimeters (mm). Under these optimized conditions, a minimum porosity of 1.8654% and a hardness value of 921 HV0.3 were achieved. Scanning electron microscopy (SEM) analysis of the cross-sectional morphology (Fig. 16). of the titania coating produced under these conditions revealed a dense and uniform structure.

Relationship between porosity and hardness

A straight line fit to the experimental data can be used to link the hardness dependency with porosity (Fig. 17). The following equation governs the straight line:

Microhardness (HV) = 1035-65.60 (Porosity) (6)

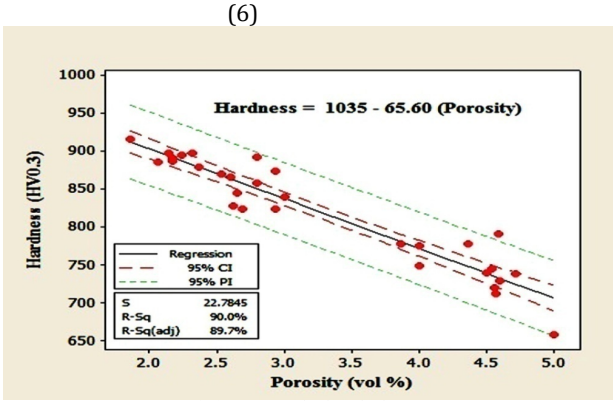

Figure 17: Relationship between Hardness and Porosity

The negative slope of the estimated regression equation (-65.60) indicates that microhardness increases as porosity decreases. The coefficient of determination (R^2 = 90%) signifies that 90% of the total variability in microhardness can be explained by the regression model, highlighting a strong goodness-of-fit. The fitted regression equation (Eq. 6) can be effectively utilized to estimate the mean microhardness for a specific coating porosity level and to predict individual microhardness values corresponding to a particular porosity.The uncertainty associated with the regression results is quantified using confidence intervals (CIs) and prediction intervals (PIs). While CIs provide an estimate of the mean value of the dependent variable (microhardness) for a given independent variable (coating porosity), PIs predict individual values and therefore exhibit a wider range due to the inherent variability in individual observations. As shown in Figure 18, the interval width narrows as the porosity value approaches 2.58%, reflecting reduced uncertainty in the estimates near this value. The ability to quantify both mean and individual estimates with appropriate intervals further validates the robustness of the regression analysis for predicting coating microhardness as a function of porosity.

Conclusions

1. This study presents the development of robust empirical models for predicting the porosity and microhardness of titania coatings deposited using the HVOF process. Key spray parameters, including fuel flow rate, oxygen flow rate, powder feed rate, and spray distance, were incorporated into the models, with fuel flow rate identified as the most influential factor governing coating properties.
2. A linear regression model with a 95% confidence level was successfully established, correlating porosity and microhardness with the identified spray parameters. Additionally, predictive models were extended to evaluate coating characteristics on titanium substrates using similar parameter inputs, enhancing the study's scope.
3. Through response surface methodology (RSM), the optimized HVOF parameters were determined as follows: oxygen flow rate of 262 lpm, fuel flow rate of

70 lpm, spray distance of 229 mm, and powder feed rate of 39 gpm. Under these optimized conditions, the coatings achieved a maximum microhardness of 921 HV0.3 and a minimum porosity of 1.86 vol%.

4. These findings provide valuable insights into the controlled deposition of high-performance titania coatings with superior mechanical properties. The optimized parameters and empirical models developed herein serve as a foundation for the precision engineering of thermal spray coatings, enabling improved performance in critical engineering applications.

References

1. Pradeep Raj. R, Thirumalaikumarasamy. D, Adarsh V Suresh, Devaki Nandhana ·P, Aravind Roy, Role of HVOF Sprayed Cermet Coatings on Improvement of Erosion - corrosion Resistance of Naval Materials - A Review, Journal of Thermal Spray and Engineering, 2024, vol 4, p 132-140
2. Oksa M, Turunen E, Suhonen T, Varis T, Hannula S-P. Optimization and Characterization of High Velocity Oxy-fuel Sprayed Coatings: Techniques, Materials, and Applications. Coatings. 2011; 1(1), p 17-52.
3. Vignesh, S., Shanmugam, K., Balasubramanian, V., & Sridhar, K. Identifying the optimal HVOF spray parameters to attain minimum porosity and maximum hardness in iron based amorphous metallic coatings. Defence technology, 2017, 13(2), 101-110.
4. Sathiyamoorthy, R., Shanmugam, K., & Balasubramanian, V. Establishing an empirical relationship to predict porosity and hardness of Titanium Oxide (TiO2) coating deposited by High Velocity Oxy Fuel (HVOF) spraying. system,2015, 8, p 10.
5. Kim, G. E., & Brochu, M. Thermal spray nanostructured ceramic and metal-matrix composite coatings. In Anti-Abrasive Nanocoatings, Woodhead Publishing, 2015, p. 481-511.
6. Sathiyamoorthy, R., Shanmugam, K., & Balasubramanian, V. EFFECTS OF HIGH VELOCITY OXY-FUEL (HVOF) PROCESS PARAMETERS ON POROSITY AND MICROHARDNESS OF TITANIA COATING. Journal of Manufacturing Engineering, 2014, 9(2), p 98-104.
7. Pawlowski. L, The science and engineering of thermal spray coatings, Wiley, 2008, 2nd ed. Chichester, West Sussex, UK.
8. Rajendran PR, Duraisamy T, Chidambaram Seshadri R, Mohankumar A, Ranganathan S, Balachandran G, Murugan K, Renjith L. Optimisation of HVOF Spray Process Parameters to Achieve Minimum Porosity and Maximum Hardness in WC-10Ni-5Cr Coatings. Coatings. 2022; 12(3), p 339.
9. Pradeep Raj. R, Thirumalaikumarasamy. D, Sonar. T, Ivanov. M , Development of slurry erosion prediction model and studying the effect of slurry erosion parameters on erosion of WC10Ni5Cr coated 35CrMo steel, International Journal on Interactive Design and Manufacturing (IJIDeM). 2023, p 1-20.
10. Mohankumar, Ashokkumar & Duraisamy, Thirumalaikumarasamy & Packkirisamy, Vignesh & Sampathkumar, Deepak. Response Surface Methodology and Mayfly Optimization for Predicting the Properties of Cold-Sprayed AA2024/Al2O3 Coatings on AZ31B Magnesium Alloy. Journal of Materials Engineering and Performance, 2023.
11. Balasubramanian, V. & Lakshminarayanan, A. & Varahamoorthy, R. & Babu, Sunkavalli. Understanding the Parameters Controlling Plasma Transferred Arc Hardfacing Using Response Surface Methodology. Materials and Manufacturing Processes, 2008, 23, p 674-682.
12. Planche, M.P. & Normand, Bernard & Liao, Hanlin & Rannou, G & Coddet, Christian. Influence of HVOF spraying parameters on in-flight characteristics of Inconel 718 particles and correlation with the electrochemical behaviour of the coating. Surface & Coatings Technology - SURF COAT TECH, 2002, 157,p 247-256.
13. K.A. Habib, D.L. Cano, José Antonio Heredia Alvaro, J. Serrano-Mira, R. Llopis, D. López Moreno, Samar S. Mohammed, Effects of thermal spraying technique on the remelting behavior of NiCrBSi coatings, Surface and Coatings Technology,2022, Volume 444, p128669.
14. Prasad, R. V., Rajesh, R., Thirumalaikumarasamy, D., Vignesh, S., & Sreesabari, S. Sensitivity analysis and optimisation of HVOF process inputs to reduce porosity and maximise hardness of WC-10Co-4Cr coatings. Sādhanā, 2021, 46, p1-23.
15. Picas, J. A., Punset, M., Baile, M. T., Martín, E., & Forn, A. Effect of oxygen/fuel ratio on the in-flight particle parameters and properties of HVOF WC-CoCr coatings. Surface and Coatings Technology, 2011, 205, p 364-368.
16. Raza, A., Ahmad, F., Badri, T. M., Raza, M. R., & Malik, K. An influence of oxygen flow rate and spray distance on the porosity of HVOF coating and its effects on corrosion—A review. Materials, 2022, 15(18), p 6329.
17. Eßler, J., Woelk, D., Utu, D., & Marginean, G. Influence of the powder feed rate on the properties of HVOF sprayed WC-based cermet coatings. Materials Today: Proceedings,2023, 78,p 227-234.
18. Kiilakoski, J., Trache, R., Björklund, S., Joshi, S., & Vuoristo, P. Process parameter impact on suspension-HVOF-sprayed Cr 2 O 3 coatings. Journal of Thermal Spray Technology, 2019, 28, p 1933-1944.
19. Mathanbabu, M., Thirumalaikumarasamy, D., & Tamilselvi, M. Optimization of plasma spray process variables to attain the minimum porosity and maximum hardness of the LZ/YSZ thermal barrier coatings utilizing the response surface approach. Materials Research Express, 2022, 9(9), p 096505.
20. Murugan, K., Ragupathy, A., Balasubramanian, V., & Sridhar, K. Optimizing HVOF spray process parameters to attain minimum porosity and maximum hardness in WC–10Co–4Cr coatings. Surface and Coatings Technology,2014, 247, p 90-102.
21. Karthikeyan, R., & Balasubramanian, V. Predictions of the optimized friction stir spot welding process parameters for joining AA2024 aluminum alloy using RSM. The International Journal of Advanced Manufacturing Technology, 2010, 51, p173-183.
22. Pradeep Raj, R., Thirumalaikumarasamy, D., Sonar, T., & Pavendhan, R. Effect of water jet erosion parameters on erosion rate of WC10Ni5Cr HVOF coated 35CrMo steel. Materials Testing,2024, 66(6), p 930-947.